European Geothermal Congress 2013
Pisa, Italy, 3-7 June 2013

Optimum configuration of plate-type heat exchangers for the use in ORCs for low-temperature geothermal heat sources

Daniël Walraven[1], Ben Laenen[2], William D'haeseleer

[1] University of Leuven (KU Leuven) Energy Institute, TME branch (Applied Mechanics and Energy Conversion), Celestijnenlaan 300A box 2421, B-3001 Leuven, Belgium

[2] Flemish Institute of Technological Research (VITO), Boeretang 200, B-2400 Mol, Belgium

Daniel.Walraven@mech.kuleuven.be, Ben.Laenen@vito.be, William.Dhaeseleer@mech.kuleuven.be

Keywords: system optimization, ORC, plate heat exchangers

ABSTRACT

Organic Rankine cycles (ORCs) are used for electricity production from low-temperature (geothermal) heat sources. These ORCs are often designed based on experience, but this experience will not always lead to the optimum configuration. The ultimate goal is to design ORCs by performing a system optimization. In such an optimization, all components and cycle parameters are optimized together to obtain the optimum power plant configuration; all components are adjusted to each other. In this paper, a first step towards such a system optimization is taken by optimizing the cycle parameters together with the configuration of the plate heat exchangers. In this way every heat exchanger has the optimum allocation of heat exchanger surface, pressure drop and pinch point temperature difference for the given boundary conditions and for use in the obtained ORC.

1. INTRODUCTION

The amount of energy stored in low-temperature geothermal heat sources is huge (Tester et al. 2006), but the conversion to electricity is inefficient due to the low temperature. Much research has been performed to maximize this conversion efficiency by the use of binary cycles (Dai et al. 2009, Saleh et al. 2007, Walraven et al. 2013). Most of these studies optimize the cycle parameters (pressures and temperatures) for different working fluids, but make assumptions about the components. Heat exchangers are assumed to be ideal or to have a fixed pressure drop, the values of pinch point temperature differences are assumed, etc. The choice of these parameters has an important influence on the performance of the ORC and on the total cost of the installation.

This issue is already touched upon in the literature. The influence of the heat exchangers was investigated by Madhawa Hettiarachchi et al. (2007). They minimized the ratio of the total heat exchanger surface and the net power produced by the cycle. The configuration of the heat exchangers was fixed. Franco and Villani (2009) divided the ORC in two levels: the system level and the component level. First, the authors optimized the system level. In a next step, they used this optimum system configuration to find the optimum configuration of the components. An iteration between both levels was needed to come to the final solution. The optimum system configuration obtained in this way will probably be very close to the one in the first iteration. To obtain the global optimum configuration of the ORC, a system optimization should be performed. In such an optimization, the system and the components are optimized together so that the components are adjusted to each other and that the components have the optimum configuration for the use in the cycle. Realistic models for all components are needed. These models should describe the performance and cost of the components as a function of some geometric parameters. Software for numerical optimization, which can deal with relatively large, strongly non-linear problems is needed.

In this paper, the first steps for a system optimization of an ORC are taken. Existing models for plate-type heat exchangers are implemented for the use as single-phase heat exchangers, condensers and evaporators. Pressure drops and heat transfer coefficients are calculated with correlations as a function of the heat exchanger geometry. These heat exchanger models are added to a previously developed ORC model, in which the heat exchangers were assumed to be ideal (Walraven et al. 2013). The software package CasADi, which is a platform for automatic differentiation and numerical optimization (Andersson et al. 2012), is used to perform the optimization.

Only simple ORCs are investigated and no other components than the heat exchangers are modeled. In fact, a platform is developed for system optimization of ORCs. Further research will extend this platform by adding extra components (shell-and-tube heat exchangers, turbine and cooling system) and by allowing other configurations of the ORC (with recuperator, with turbine bleeding and multi-pressure cycles)

2. THERMODYNAMIC CYCLE

Figure 1 shows the scheme of a simple ORC. The working fluid is pumped to a high pressure (1→2), heated by the brine in the economizer, evaporator and superheater (2→6), expanded in the turbine (6→7) and cooled in the desuperheater and condenser. The numbers of the states are the same as used in Walraven et al. (2013).

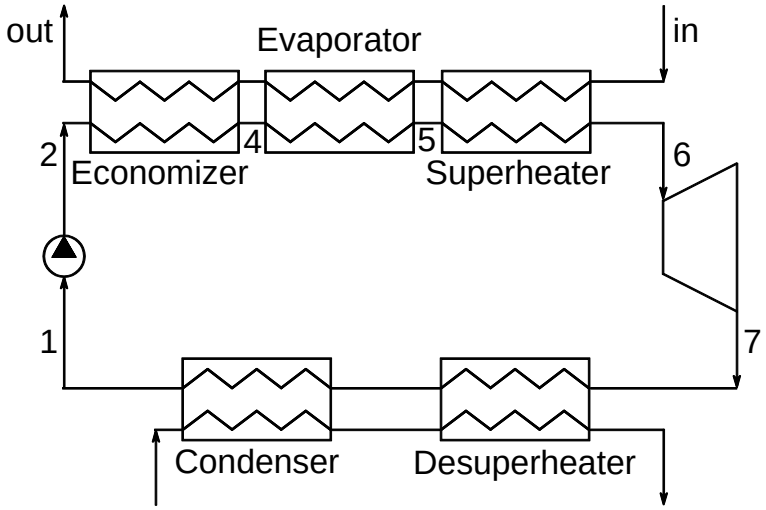

Figure 1: Scheme of an ORC with the different heat exchangers. The state points are the same as in (Walraven et al. 2013).

In figure 1, 5 heat exchangers are shown, but not all of them have to be used. When the working fluid is a dry one, often no superheater is needed. An ORC with a wet fluid often does not have a desuperheater and transcritical cycles do not need an evaporator.

State 1 is saturated liquid, state 6 can be saturated or superheated vapor and the cycle can be subcritical or transcritical. More information can be found in Walraven et al. (2013), in which the cycle is described. In this paper, the power needed to compensate the pressure drop in the brine and cooling water is also taken into account.

It is assumed that the pumps and the turbine have a fixed isentropic efficiency of 80 and 85%, respectively. The models for the heat exchangers are given in section 3. With these models, the heat transfer coefficient and pressure drop can be calculated, depending on the geometry of the heat exchangers. These geometries will be optimized, together with the parameters of the cycle (temperatures and pressures).

3. PLATE HEAT EXCHANGERS

In order to find the optimum configuration of the heat exchangers used in the cycle, models which describe the performance of the heat exchangers as a function of the configuration are needed. Models for single-phase heat exchangers, evaporators and condensers are found in the literature and are described below.

3.1 Single-phase

Martin (1996) has developed a model for plate-type heat exchangers with chevron-type corrugations in which many geometrical parameters are included. These parameters are shown in figure 2.

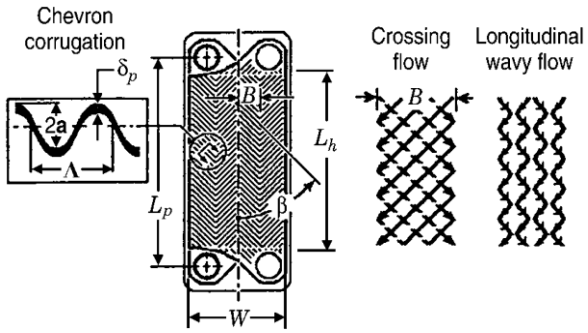

Figure 2: Geometrical parameters of the chevron-type heat exchanger (Martin 1996).

The corrugations are determined by the amplitude a, the width Λ and the angle of the corrugations β. The hydraulic diameter is then defined as:

$$D_h = {}^{4a}/_{\Phi} \qquad [1]$$

with Φ the ratio of the total area of the plate to the projected area. This ratio is given by:

$$\Phi \approx \tfrac{1}{6}(1 + \sqrt{1 + X^2} + 4\sqrt{1 + X^2/2}) \qquad [2]$$

in which the dimensional corrugation parameter X is defined as:

$$X = 2\pi a/\Lambda \qquad [3]$$

The total pressure drop in the heat exchanger is given by:

$$\Delta p = \frac{\xi L_p}{D_h}\frac{\rho v^2}{2} \qquad [4]$$

with ξ the Darcy friction coefficient, L_p the length of the plate between the inlet and outlet port, ρ the density of the fluid and v the velocity of the fluid.

Martin (1996) obtained the following formula for the friction coefficient:

$$\frac{1}{\sqrt{\xi}} = \frac{\cos\beta}{\sqrt{b\tan\beta + c\sin\beta + \xi_0/\cos\beta}} + \frac{1-\cos\beta}{\sqrt{\xi_1}} \quad [5]$$

ξ_0 and ξ_1 are the Darcy friction coefficient in the case β is equal to zero and 90°, respectively. These coefficients are given by:

$$\xi_0 = \frac{64}{Re} \qquad Re < 2000 \quad [6]$$

$$\xi_0 = (1.8\log Re - 1.5)^{-2} \qquad Re \geq 2000 \quad [7]$$

and

$$\xi_1 = \frac{597}{Re} + 3.85 \qquad Re < 2000 \quad [8]$$

$$\xi_1 = \frac{39}{Re^{0.289}} \qquad Re \geq 2000 \quad [9]$$

where Re is the Reynolds number based on the hydraulic diameter.

The parameters a, b and c are obtained by comparing equation [5] with experiments. The optimum values according to Martin (1996) are 3.8, 0.18 and 0.36, respectively.

The correlation for the Nusselt number is:

$$Nu = 0.122 Pr^{\frac{1}{3}} \left(\frac{\eta}{\eta_w}\right)^{1/6} [\xi Re^2 \sin(2\phi)]^{0.374} \quad [10]$$

with Pr the Prandtl number, η the viscosity and η_w the viscosity at the wall temperature.

3.2 Evaporator

Han et al. (2003a) developed correlations for the Nusselt number and pressure drop for evaporation in plate heat exchangers with chevron-type corrugations which depend on the geometrical configuration of the exchanger.

The Nusselt number is calculated as:

$$Nu = Ge_1 Re_{eq}^{Ge_2} Bo_{eq}^{0.3} Pr_f^{0.4} \quad [11]$$

Ge_1 and Ge_2 are non-dimensional geometric parameters. Re_{eq} and Bo_{eq} are the equivalent Reynolds and boiling number, respectively. These parameters and numbers are given by:

$$Ge_1 = 2.81 \left(\frac{\Lambda}{D_h}\right)^{-0.041} \beta^{-2.83} \quad [12]$$

$$Ge_2 = 0.746 \left(\frac{\Lambda}{D_h}\right)^{-0.082} \beta^{0.61} \quad [13]$$

$$Re_{eq} = \frac{G_{eq} D_h}{\mu_f} \quad [14]$$

$$Bo_{eq} = \frac{q}{G_{eq} h_{fg}} \quad [15]$$

μ_f is the viscosity of the saturated liquid, q the heat flux, h_{fg} the enthalpy of evaporation and G_{eq} the equivalent mass flux, given by:

$$G_{eq} = G\left[1 - x + x\left(\frac{\rho_f}{\rho_g}\right)^{1/2}\right] \quad [16]$$

with G the total mass flux, x the quality of the two-phase fluid and $\rho_g$the density of the saturated vapor.

The frictional pressure drop is calculated as:

$$\Delta p_{fr} = f \frac{L_p}{D_h} \frac{G_{eq}^2}{\rho_f} \quad [17]$$

with f the two-phase friction factor and ρ_f the density of the saturated liquid.

The two-phase friction factor f is calculated as:

$$f = Ge_3 Re_{eq}^{Ge_4} \quad [18]$$

where the non-dimensional geometric parameters Ge_3 and Ge_4 are given by:

$$Ge_3 = 64710 \left(\frac{\Lambda}{D_h}\right)^{-5.27} \beta^{-3.03} \quad [19]$$

$$Ge_4 = -1.314 \left(\frac{\Lambda}{D_h}\right)^{-0.62} \beta^{-0.47} \quad [20]$$

3.3 Condenser

The correlations for the condenser are given by Han et al. (2003b). The correlation for the Nusselt number is:

$$Nu = Ge_1 Re_{eq}^{Ge_2} Pr_f^{1/3} \quad [21]$$

with

$$Ge_1 = 11.22 \left(\frac{\Lambda}{D_h}\right)^{-2.83} \beta^{-4.5} \quad [22]$$

$$Ge_2 = 0.35 \left(\frac{\Lambda}{D_h}\right)^{0.23} \beta^{1.48} \quad [23]$$

The equivalent Reynolds number is given by equation [14].

The frictional pressure drop is calculated from equation [17]. The correlation for the condensation friction factor is:

$$f = Ge_3 Re_{eq}^{Ge_4} \quad [24]$$

The non-dimensional geometric parameters are given as:

$$\mathrm{Ge}_3 = 3521.1\left(\frac{\Lambda}{\mathrm{D_h}}\right)^{4.17}\beta^{-7.75} \quad [25]$$

$$\mathrm{Ge}_4 = -1.024\left(\frac{\Lambda}{\mathrm{D_h}}\right)^{0.0925}\beta^{-1.3} \quad [26]$$

4. OPTIMIZATION

The objective of the optimization is to maximize the net power produced by the power plant. This power is defined as:

$$\dot{W}_{net} = \dot{W}_{turbine} - \dot{W}_{pump}^{ORC} - \dot{W}_{pump}^{cooling} - \dot{W}_{pump}^{brine} \quad [27]$$

$$\dot{W}_{turbine} = \dot{m}_{WF}(h_6 - h_7) \quad [28]$$

$$\dot{W}_{pump}^{ORC} = \dot{m}_{WF}(h_2 - h_1) \quad [29]$$

$\dot{m}_{WF}$ is the mass flow of the working fluid, h_x is the enthalpy of the working fluid in state x. $\dot{W}_{pump}^{cooling}$ and $\dot{W}_{pump}^{brine}$ are the power needed to overcome the pressure drop of the cooling water and the brine, respectively.

The decision variables are the temperature and pressure at the inlet of the turbine (state 6 in figure 1), the pressure at state 1, the mass flow of the working fluid and the geometric parameters of each of the 5 heat exchangers. These parameters are the corrugation amplitude, the corrugation width, the corrugation angle and the length of the plate. So, there are in total 24 decision variables.

A non-linear inequality constraint is added to the problem: the heat exchanger surface of all heat exchangers should be smaller or equal to a maximum surface A_{max}. The heat exchangers represent a large part of the total cost of the ORC. The cost of a heat exchanger depends strongly on its surface (Madhawa Hettiarachchi et al. 2007). So, A_{max} is representative for the cost of the installation. The optimizer can choose how to distribute this allowed heat exchanger surface amongst the different heat exchangers, in order to obtain an exergetic plant efficiency as high as possible. The influence of the value of A_{max} is also investigated.

The optimization is performed by the optimization software CasADi (Andersson et al. 2012). This is a symbolic framework for automatic differentiation and numeric optimization. The software itself chooses to use automatic differentiation in forward or reverse/adjoint mode. For the problem in this paper, the software chooses for the reverse mode. The advantage of this mode is that the gradient of the objective function and the non-linear constraint are calculated much faster and more accurately than a gradient calculated by finite-differences.

The fluid properties are obtained from REFPROP (Lemmon et al. 2007) and the complex-step derivative method (Martins et al. 2003) is used to obtain the gradient of these fluid properties. This gradient is used by CasADi to calculate the gradients of the objective function and the non-linear constraints. The connection between Fortran and Python is made by F2PY (Peterson 2009).

5. RESULTS AND DISCUSSION

Table 1 shows the parameters which are used in the remainder of the paper, unless denoted otherwise.

Table 1: Input parameters

A_{max}	40m²/kg/s-brine
Brine inlet temperature	125°C
Brine inlet pressure	10 bar
Cooling water mass flow	10 kg/s-water/kg/s-brine
Cooling water inlet temperature	15°C

5.1 Influence of A_{max}

In this section, the influence of the total allowed heat exchangers surface is investigated. Figure 3 shows the net power output for different working fluids as a function of the maximum allowed heat transfer surface. Calculations have been performed for all fluids available in REFPROP, for which the transport properties are available and for which a subcritical or transcritical cycle is possible. In the remainder of the paper, only some promising and widely used fluids are shown for clarity.

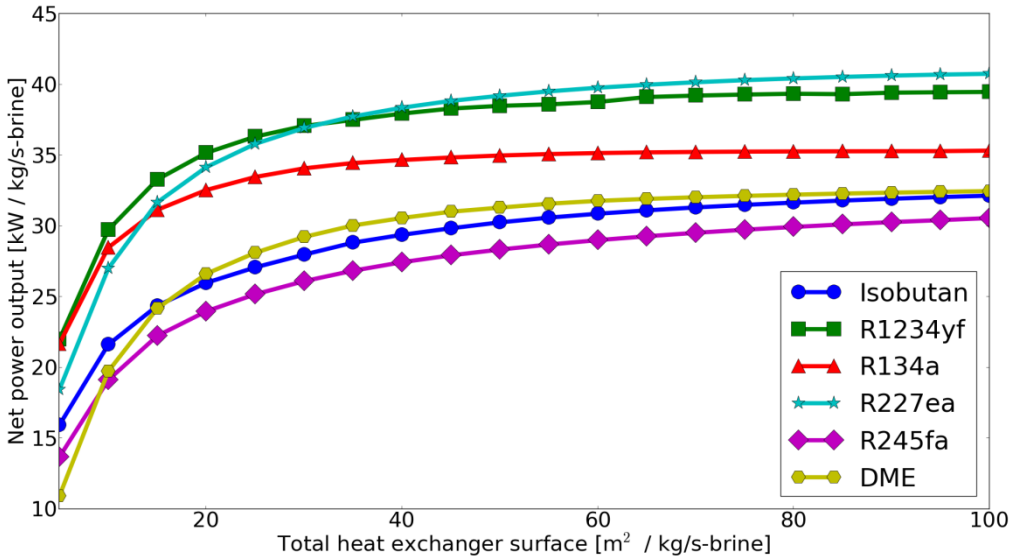

Figure 3: Net power output of the ORC for different working fluids, as a function of the maximum allowed heat transfer surface

The net power output increases with maximum allowed heat exchanger surface as expected. The point at which adding extra heat exchanger surface does not seem to be useful, varies between 20 to 40 m²/kg/s-brine. For a subcritical cycle like the ones with isobutane and DME, this point lies at relatively low heat exchanger surfaces, while for a transcritical cycle with R227ea, this point lies at higher heat exchanger surfaces. This is explained by the minimum temperature difference between brine and working fluid, as shown in figure 4.

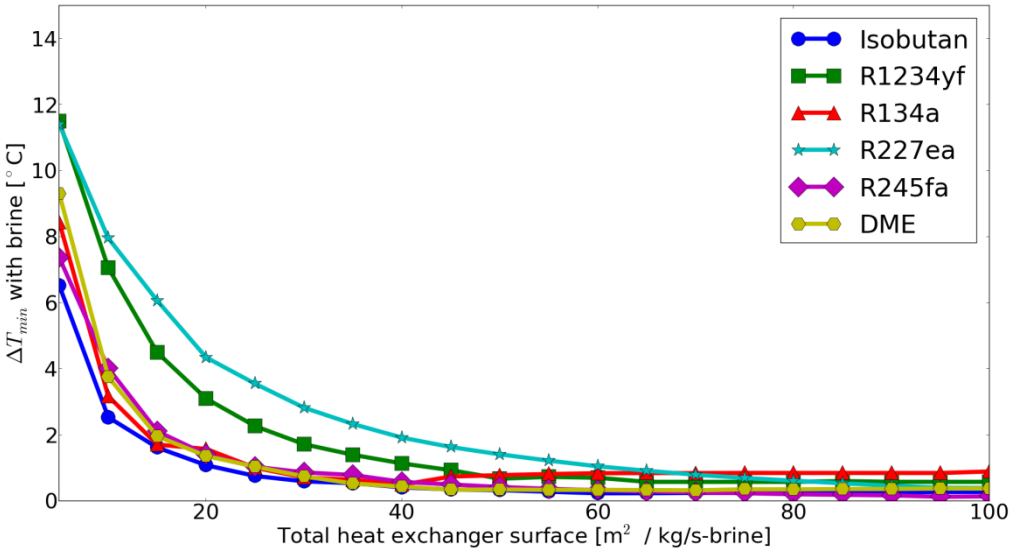

Figure 4: Minimum temperature difference between the brine and working fluid for different fluids, as a function of the maximum allowed heat transfer surface

The minimum temperature difference between the brine and the working fluid is always relatively low (<10°C) for isobutane and DME. These cycles are subcritical, so the pinch point exists at the entrance of the evaporator. The temperature difference between the working fluid and brine in the economizer, the evaporator and potentially in the superheater are relatively high. So, the average temperature difference between the fluids is relatively high. For a transcritical cycle (R227ea and R1234yf), the fit between the working fluid heating curve and the brine cooling curve is much better. The average temperature difference between the fluids will therefore be closer to the minimum one than in a subcritical cycle. This minimum temperature difference is therefore larger in a transcritical cycle than in a subcritical one.

The minimum temperature difference between the working fluid and the cooling water is shown in figure 5. This temperature difference is very similar for all working fluids. For a subcritical cycle, the minimum temperature difference between brine and working fluid is lower than the temperature difference between working fluid and cooling water. For a transcritical cycle, both temperature differences are about the same. This is because the fit between the cooling water heating curve and the working fluid cooling curve is relatively good. For a subcritical cycle, this fit is better than the fit between brine and working fluid, for the transcritical cycles, both fits are about the same.

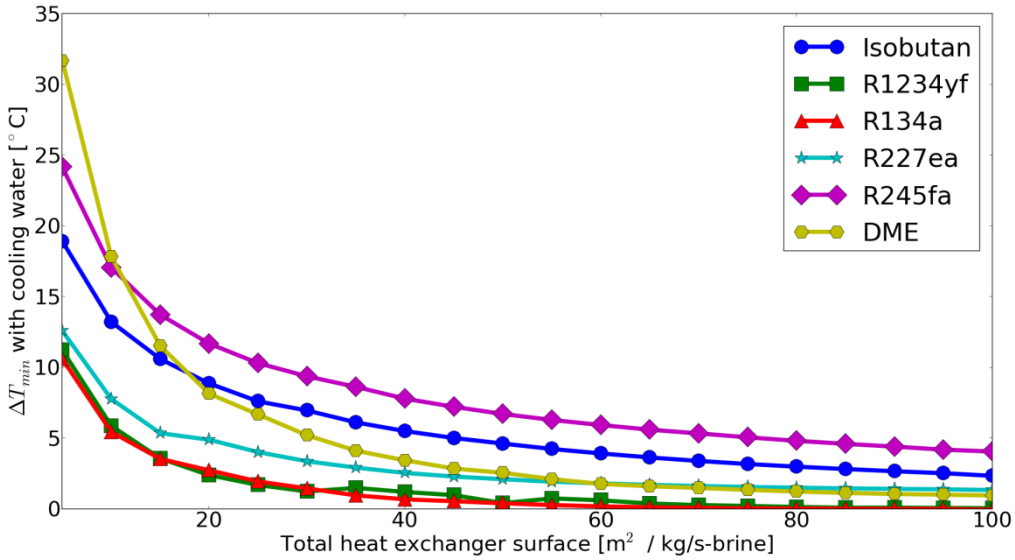

Figure 5: Minimum temperature difference between the working fluid and the cooling water for different fluids, as a function of the maximum allowed heat transfer surface

5.2 Influence of the cooling water inlet temperature

In this section the reference input parameters of table 1 are used, but the cooling water temperature is varied between 5 and 40°C. For every cooling water inlet temperature a new optimum configuration is calculated. The net power produced by the ORC decreases almost linearly with increasing cooling water inlet temperature as shown in figure 6. This linear decrease is already mentioned by Walraven et al. (2013), but the effect in this paper is less. This is because the configuration of the heat exchangers is adapted: the heat transfer coefficient is increased when the cooling water inlet temperature increases to obtain lower temperature differences in the heat exchangers as shown in figures 7 and 8. As a consequence the pressure drop in the heat exchangers increases, but the electric power needed to compensate for this is apparently less than the gain of electric power in the turbine by decreasing the temperature differences in the heat exchangers.

The discontinuities in the slope of the curves of R227ea for cooling water inlet temperatures between 15 and 20°C exists because of the transition of a subcritical to a transcritical cycle. For an increasing cooling water inlet temperature, the temperature difference between the brine and the working fluid decreases. So, the maximum pressure of the working fluid has to increase and will become supercritical at a certain moment. The strong drop in the minimum temperature differences for R1234yf is also caused by a change in configuration of the cycle.

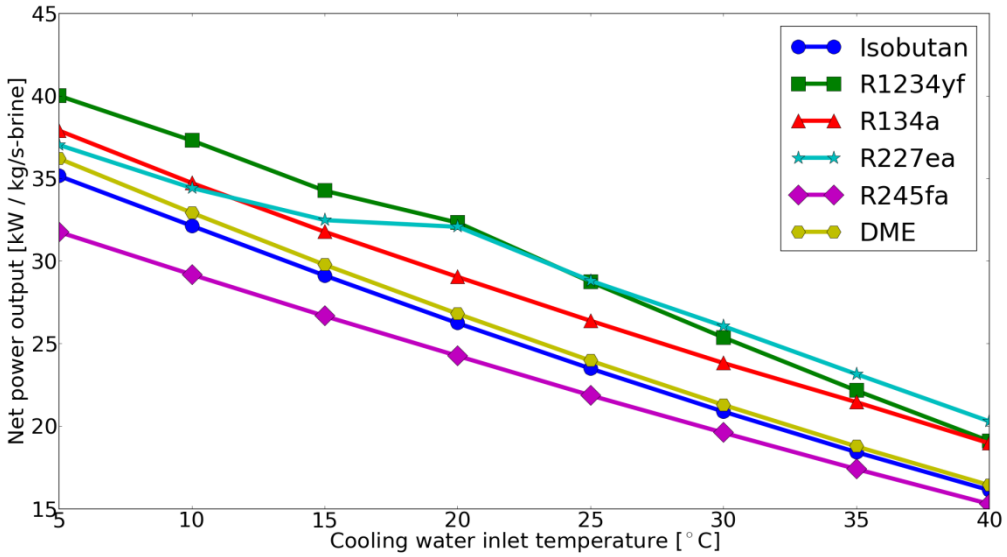

Figure 6: Net power output of the ORC for different working fluids, as a function of the cooling water inlet temperature.

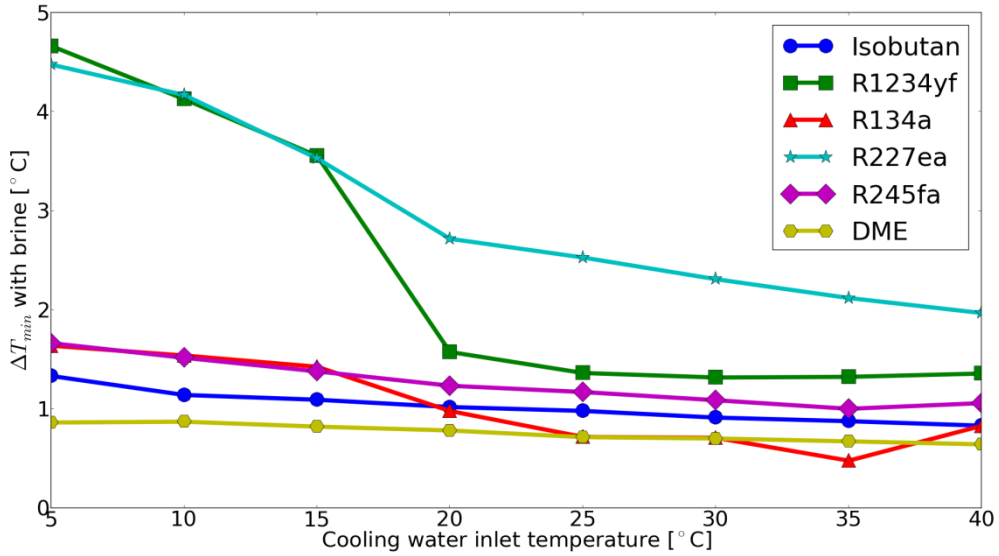

Figure 7: Minimum temperature difference between the brine and working fluid for different fluids, as a function of the cooling water inlet temperature

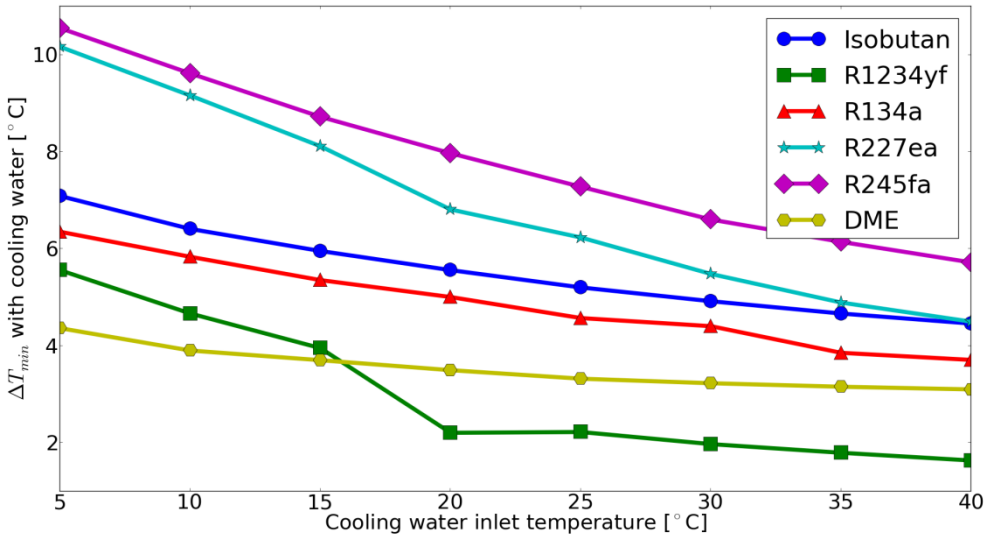

Figure 8: Minimum temperature difference between the working fluid and the cooling water for different fluids, as a function of the cooling water inlet temperature

5.3 Influence of the cooling water mass flow

In this section, the influence of the cooling water mass flow is investigated. The input parameters are given in table 1, but the cooling water mass flow is varied between 2 and 20 kg/s-water / kg/s-brine. The net power output is shown in figure 9. The power output does not keep increasing with increasing cooling water mass flow, but there is an optimum value of the cooling water mass flow. The value of this optimum mass flow depends on the fluid used. For low cooling water mass flows, the cooling water heats up strongly and the condensing temperature is therefore high. For high cooling water mass flows, the velocity of the cooling water in the heat exchanger becomes high and so does the pressure drop. At a certain mass flow, the electric power needed to overcome this pressure drop becomes larger than the extra electric power obtained by reducing the condensing temperature.

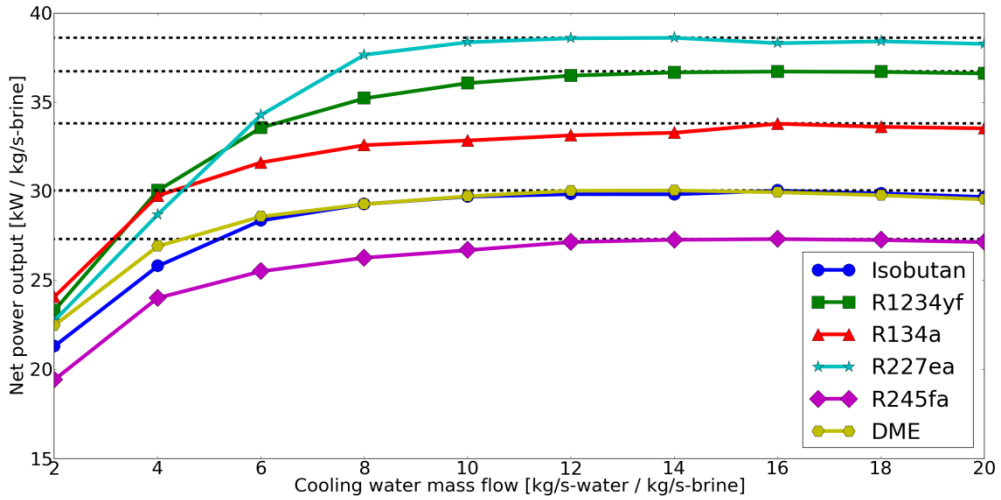

Figure 9: Net power output of the ORC for different working fluids, as a function of the cooling water mass flow. The dashed horizontal lines represent the maximum net power output for each fluid.

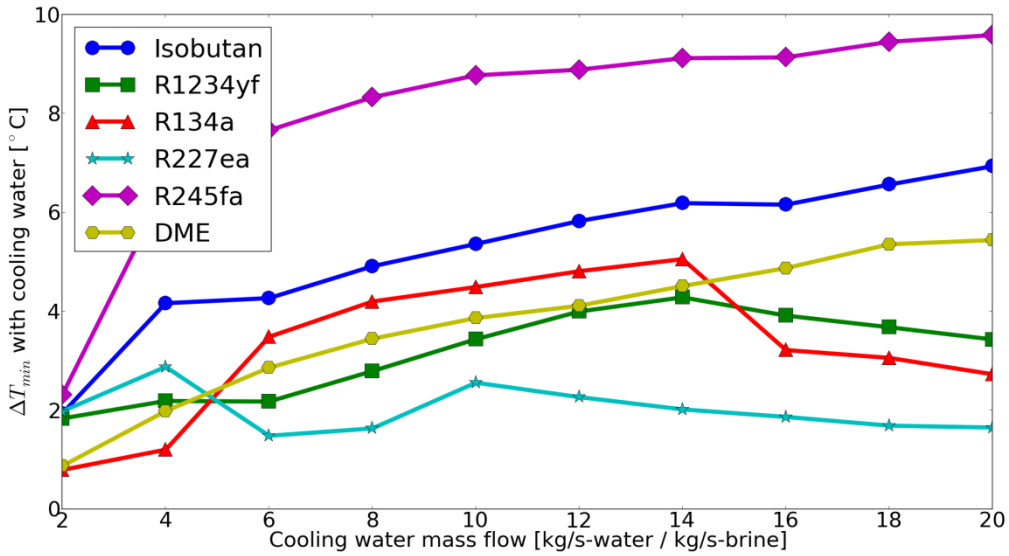

Figure 10: Minimum temperature difference between the working fluid and the cooling water for different fluids, as a function of the cooling water mass flow

The minimum temperature difference between the brine and the working fluid remains more or less constant, but the minimum temperature difference between working fluid and cooling water increases with increasing cooling water mass flow for the subcritical cycles (isobutane, R245fa, DME) as shown in figure 10. When the cooling water mass flow increases, it will heat up less. The average temperature difference between working fluid and cooling water will therefore be closer to the minimum one. The average temperature difference is more or less constant and the minimum temperature difference increases. For R1234yf, R134a and R227ea the cycle configuration changes strongly and the evolution of

the minimum temperature differences is strongly dependent on the configuration.

6. CONCLUSIONS

A platform for system optimization of ORCs is developed. This platform is used to find the optimum configuration of a simple ORC and the different plate-type heat exchangers needed in the ORC. The models for the heat exchangers are found in the literature.

It is shown that the first step towards a system optimization works. It is also shown that the influence of many parameters (cooling water temperature and mass flow, allowed heat exchanger surface) is very strong and depends on the type of working fluid.

The platform will be extended in further research by adding models of shell-and-tube heat exchangers, turbines and cooling systems. ORCs with recuperators, turbine bleeding and multi-pressure levels will be added. The final goal is to extend the platform in such a way that the economically most optimum configuration of ORCs can be calculated based on the site-specific conditions.

REFERENCES

Andersson, J., Åkesson, J. and Diehl, M.: CasADi – A symbolic package for automatic differentiation and optimal control, in: Recent Advances in Algorithmic Differentiation, **87**, 297-307, *Springer Berlin Heidelberg*, (2012)

Dai, Y., Wang, J. and Gao, L.: Parametric optimization and comparative study of organic Rankine cycle (ORC) for low grade waste heat recovery, *Energy Conversion and Management*, **50**, (2009), 576-582

Franco, A., Villani, M.: Optimal design of binary cycle power plants for water-dominated, medium-temperature geothermal fields, *Geothermics*, **38**, (2009), 379-391

Han, D.-H., Lee, K.-J. and Kim, Y.-H.: Experiments on the characteristics of evaporation of R410A in brazed plate heat exchangers with different geometric configurations, *Applied Thermal Engineering*, **23**, (2003), 1209-1225

Han, D.-H., Lee, K.-J. and Kim, Y.-H.: The Characteristics of Condensation in Brazed Plate Heat Exchangers with Different Chevron Angles, *Journal of the Korean Physical Society*, **43**, (2003), 66-73

Lemmon, E., Huber, M., Mclinden, M.: NIST reference fluid thermodynamic and transport properties REFPROP, The National Institute of Standards and Technology (NIST), Version 8.0, (2007)

Madhawa Hettiarachchi, H.D., Golubovic, M., Worek, W.M. and Ikegami, Y.: Optimum design criteria for an Organic Rankine cycle using low-temperature geothermal heat sources, *Energy*, **32**, (2007), 1698-1706

Martin, H.: A theoretical approach to predict the performance of chevron-type plate heat exchangers, *Chemical Engineering and Processing*, **35**, (1996), 301-310

Martins, J.R.R.A., Sturdza, P. and Alonso, J.J.: The Complex-Step Derivative Approximation, *ACM Transactions on Mathematical Software*, **29**, (2003), 245-262

Peterson, P., F2PY: a tool for connecting Fortran and Python programs, *International Journal of Computer Science Engineering*, **4**, (2009), 296-305

Saleh, B., Koglbauer, G., Wendland M. and Fischer, J.: Working fluids for low-temperature organic Rankine cycles, *Energy*, **32**, 1210-1221, (2007)

Tester, J., Anderson, B., Batchelor, A., Blackwell, D., DiPippo, R., Drake, E., Garnish, J., Livesay, B., Moore, M. and Nichols, K.: The Future of Geothermal Energy: Impact of Enhanced Geothermal Systems (EGS) on the United States in the 21st Century, *MIT*, Massachusetts, USA, (2006)

Walraven, D., Laenen, B. and D'haeseleer, W.: Comparison of thermodynamic cycles for power production from low-temperature geothermal heat sources, *Energy Conversion and Management*, **66**, (2013), 220-233

Acknowledgements

Daniël Walraven is supported by a VITO doctoral grant. The valuable discussions on optimization with Joris Gillis (KU Leuven) are gratefully acknowledged and highly appreciated.